6.6 AEROSOL INDIRECT EFFECTS AND RADIATIVE-DYNAMICAL FEEDBACKS IN THIN STRATOCUMULUS

J.L. Petters*
Earth and Planetary Sciences Department, University of Californa - Santa Cruz

Jerry Y. Harrington and Eugene E. Clothiaux
Department of Meteorology, Pennsylvania State University

Howard W. Barker and Jason N.S. Cole
Environment Canada

1.. Introduction

Boundary-layer stratiform clouds are persistent and prevalent Klein and Hartmann (1993), imparting a strong negative forcing to the Earth's radiative budget (Chen et al. 2000). The representation of these clouds in current climate models is relatively poor, leading to large uncertainty in climate projections [Randall et al. (2007); Intergovernmental Panel on Climate Change (IPCC)]. This problem is exacerbated by the sensitivity of stratiform clouds to perturbations in aerosol concentrations which impact cloud evolution and subsequently alter the Earth's radiative budget. Twomey (1977) showed that an increase in cloud aerosol concentrations leads to higher cloud droplet number concentrations (N_d), increasing cloud reflectivity and thus reducing the solar heating of the surface (the *first aerosol indirect effect*, or first AIE). Evidence for this effect has been found in satellite observations of stratocumulus impacted by aerosol and moisture from ship tracks (e.g., Coakley et al. 1987).

Twomey (1977) considered static clouds, however. When N_d increases the cloud can thin or thicken through various dynamic feedbacks, altering the cloud radiative response (*second aerosol indirect effects*). Albrecht (1989), for instance, hypothesized that an increase in N_d can reduce the efficiency of the collection process, reducing precipitation and increasing both vertically integrated cloud liquid water (liquid water path, or LWP) and cloud lifetime. Subsequent studies have shown that the opposite of Albrecht's hypothesis can also occur. For example, increasing N_d can lead to reductions in LWP when low relative humidity air resides above the boundary layer (Ackerman et al. 2004).

While AIEs in stratiform clouds have been extensively studied with models (e.g., Ackerman et al. 2004; Lu and Seinfeld 2005; Wood 2007; Sandu et al. 2008; Hill et al. 2008) and observations (e.g., Durkee et al. 2000; Lu et al. 2007), AIEs for low LWP stratiform clouds have been essentially ignored. Unlike thicker stratocumulus, cloud top longwave cooling is sensitive to both LWP and N_d in low LWP ($< 50\,\mathrm{g\,m^{-2}}$) clouds (e.g. Garrett and Zhao 2006). Longwave cooling drives circulations that help maintain stratiform clouds (e.g., Lilly 1968; Nicholls 1984); therefore changes in longwave cooling caused by AIEs can alter the dynamic driving force and cloud lifetime. While some modeling studies of low LWP clouds have been done (e.g. Lee et al. 2009), none have examined radiative-dynamic feedbacks to AIEs.

AIE feedbacks could be climatically important because low LWP clouds are prevalent in both satellite and ground-based remote sensing data (Turner et al. 2007). Stratiform cloud layers with LWP $< 50\,\mathrm{g\,m^{-2}}$ have been observed in both mid (Lu et al. 2007; Brunke et al. 2010) and high latitudes (De Boer et al. 2009). The Arctic is frequently covered with low LWP clouds. Perturbations in Arctic cloud amounts have been linked to the recent changes in sea-ice extent (Francis and Hunter 2006; Kay et al. 2008), an important regulator of the Earth's climate. An environment with low aerosol concentrations like the Arctic (Curry et al. 1996) could be susceptible to AIEs.

Here we explore the nighttime and daytime evolution of low LWP ($< 50\,\mathrm{g\,m^{-2}}$) stratiform clouds, and how this evolution varies with N_d, using large-eddy simulation (LES). We find that an increase in N_d leads to cloud thinning at night and cloud dissipation during the day. These findings suggest a new second aerosol indirect effect, particular to low LWP stratiform clouds, that may play a role in Earth's climate.

2.. Cloud Integrated Radiative Heating

Evolution of stratocumulus is dependent, in part, on radiative heating which drives the cloud dynamics. Generally, greater longwave cooling drives stronger circulations and may produce thicker, longer lasting clouds whereas greater shortwave warming has the opposite effect (e.g., Nicholls 1984). Radiative heating feeds back on other cloud processes (e.g. drizzle) and alters cloud evolution (Bretherton et al. 2004). Radiative heating depends primarily on the cloud LWP and N_d. Moreover, to first order cloud dynamics respond to cloud vertically integrated radiative heating (what we will call the *total* radiative warming or cooling) of the layer (e.g., Lilly 1968; Wood 2007). Computations of total radiative heating for static clouds, there-

**Corresponding author address:* Jonathan L. Petters, UC - Santa Cruz, Earth and Marine Sci., Santa Cruz, CA 95064.
E-mail: jlpetter@ucsc.edu

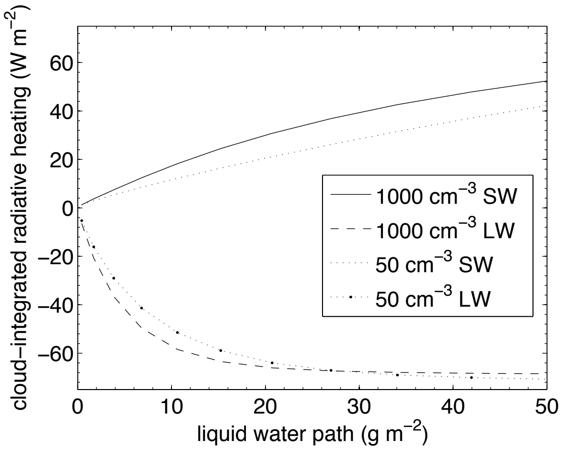

FIG. 1. Total cloud shortwave heating and longwave cooling as a function of LWP for low-altitude stratiform clouds with an adiabatic liquid water content. A perturbation in aerosol amount is emulated using two drop concentrations: $N_d = 50\,\mathrm{cm}^{-3}$ and $1000\,\mathrm{cm}^{-3}$. Total shortwave radiative heating was computed with a solar zenith angle of $\Theta = 0\ ^\circ$. Shortwave heating varies with Θ but for simplicity we show $\Theta = 0\ ^\circ$ (overhead sun) because other values of Θ give qualitatively similar results.

fore, provide a framework to interpret our AIE results in LES.

We created static atmospheres by adding a cloud-topped boundary layer to the the mid-latitude summer (MLS) sounding of McClatchey et al. (1972). We specified cloud base as 1 km and varied cloud top with an adiabatic liquid water content (LWC) allowing variations in LWP (Petters 2009). We assumed drop concentration N_d mixing-ratios were constant-in-height which closely resembles profiles typically observed in these clouds (Miles et al. 2000).

For consistency, we employ the same two-stream solver as is used in the LES [Harrington (1997) which is based on Ritter and Geleyn (1992)]. Gaseous absorption in the shortwave and longwave is modeled using the correlated-k distribution (CKD) spectral band model (27 shortwave and 12 longwave intervals) as described in Cole (2005). Cloud optical properties are modeled using the binned approach described in Harrington and Olsson (2001) and are held constant over each wavelength interval.

We expect AIE feedbacks when radiative heating is sensitive to changes in LWP or N_d. The amount of total cloud radiative warming or cooling is most dependent on the LWP and less dependent on perturbations in N_d (Fig. 1). We find little variation in total longwave cooling with LWP or N_d for clouds with LWP $> 20\,\mathrm{g\,m}^{-2}$; hence consistent with Garrett and Zhao (2006), we expect no AIE longwave feedbacks to occur for these thicker clouds. However, for lower LWPs the total longwave cooling is sensitive to changes in LWP and N_d; the LWP sensitivity is even stronger than for shortwave warming. *This result indicates that longwave AIEs likely operate in only the thinnest of clouds.*

Unlike longwave cooling, total shortwave warming (shown for $\Theta = 0\ ^\circ$, or overhead sun, only in Fig. 1) shows sensitivity to N_d for all LWP $< 50\,\mathrm{g\,m}^{-2}$ and continues to increase with LWP. Total shortwave warming rises with an increase in drop concentration, as shown by Boers and Mitchell (1994). *Consequently, when shortwave warming is strong, we expect AIE effects related to this warming for the entire range of low LWPs.* As we show below, the different response of longwave and shortwave heating to changes in LWP have important consequences for the evolution of low LWP clouds under different perturbations in aerosol amount.

3.. Dynamical Atmospheric Model

We examine radiative-dynamical feedbacks induced by AIEs in low LWP clouds using the Regional Atmospheric Modeling System (RAMS) version 4.3.0 (Cotton et al. 2003) in LES mode (see Stevens et al. 1998; Jiang et al. 2002). We configure the model for 70 grid-points with 50 m horizontal spacing and 95 grid-points with 30 m vertical spacing, making a modeling domain of 3.40 km on a side and 2.79 km in height. Entrainment of cloud-free air into the stratocumulus topped boundary layer (STBL) plays a significant role in stratiform cloud dynamics (e.g., Lilly 1968). While relatively accurate representations of entrainment with LES require higher vertical resolution than used here, relative comparisons between our simulations are valid (Bretherton et al. 1999).

Our model timestep is 2 s and, following Xu and Randall (1995), we set our radiative timestep at 6 s to avoid spatial correlation errors between radiative heating and evolving cloud properties. We use the bulk cloud microphysical scheme of Meyers et al. (1997), predicting both mass and number concentration of drizzle. However, cloud drop number concentration is fixed during a simulation, hence feedbacks between changes in drop concentration and dynamics do not occur. As a consequence, all AIEs occur through an initial change in N_d. This is a limitation, but should provide a qualitative first-order estimate of the radiative-dynamic response.

We initialize the model with random thermal perturbations to an input sounding that produces thick stratiform clouds (Hartman and Harrington 2005). A low LWP stratiform cloud was created by lowering the vapor mixing ratio by 2.75 $\mathrm{g\,kg}^{-1}$ above the boundary layer inversion. Entrainment warming and drying then quickly leads to a thin, broken cloud.

To illustrate longwave and shortwave AIEs, we conduct simulations of both a nocturnal and a diurnal (daytime) case. We emulate aerosol perturbations with three different constant cloud droplet concentrations of $50\,\mathrm{cm}^{-3}$, $200\mathrm{cm}^{-3}$ and $1000\,\mathrm{cm}^{-3}$. The nocturnal case is six hours long whereas the daytime case is sixteen hours in length to capture the diurnal cycle in solar heating. We start the simulations with $N_d = 50\,\mathrm{cm}^{-3}$ and $1000\,\mathrm{cm}^{-3}$ at the end of the first hour of the $N_d = 200\,\mathrm{cm}^{-3}$ simulation to avoid differences in model spin-up.

4.. Results - Nocturnal Simulations

Substantial differences occur in our nocturnal simulations due to varying N_d. Averaged over the last two hours of six hour simulation time the LWPs for our simulations with $50\,\mathrm{cm}^{-3}$, $200\mathrm{cm}^{-3}$ and $1000\,\mathrm{cm}^{-3}$ are $31.7\,\mathrm{g\,m}^{-2}$, $20.4\,\mathrm{g\,m}^{-2}$ and $14.9\,\mathrm{g\,m}^{-2}$ respectively (Fig. 2a). Cloud fractions, defined as the ratio of model columns with LWP $> 10\,\mathrm{g\,m}^{-2}$ to the total number of model columns, also decrease substantially as N_d increases (Fig. 2a). As Fig. 1 indicates, the decrease in LWP leads to reductions in total longwave cooling (Fig. 2b). An additional reduction in total longwave cooling is due to averaging-in grid cells that lack clouds. Larger N_d leads to lower LWPs and hence weaker cloud circulations, as the boundary-layer averaged Turbulent Kinetic Energy (TKE) shows (Table 1; tables are at the end of this document).

How do increases in N_d produce decreases in LWP? Because the simulations diverge immediately, the first hour is critical to explaining the differences. A strong drizzle process can change TKE (Stevens et al. 1998); however the vertically integrated drizzle flux divergence (converted to an energy flux, Table 1) is small in comparison to the total longwave cooling (Fig. 2b). The drizzle fluxes are consequently weak and so do not play a role in altering the energetics of the cloud layer. Direct changes in total longwave cooling also cannot be the reason, because if they were the dominant process LWP would increase since more cooling leads to greater drop growth. The only process left that can explain the initial differences is entrainment.

Increasing N_d in stratocumulus leads to smaller drops that can evaporate more readily. Wang et al. (2003) and Hill et al. (2008) have demonstrated that an increase in N_d leads to increased evaporational cooling through entrainment and hence reductions in LWP. Hill et al. (2009) termed this process the "evaporation-entrainment feedback" and it is the reason for the initial reduction in LWP with increases in N_d. In our case, cloud fractions are also reduced through this feedback because LWP is low.

The model dynamics in our three simulations are identical when they begin and therefore the modeled entrainment is also identical. This means that initial mixing of air across the cloud-top interface is similar amongst the three simulations, and leads to larger reductions in LWP and cloud fraction as N_d is increased. The LWPs and cloud fractions are reduced to different amounts concomitant with reductions in N_d and are then associated with differing amounts of total longwave cooling. For $N_d = 1000\,\mathrm{cm}^{-3}$ the total longwave cooling is sufficiently reduced to result in a thin broken cloud layer in which LWP decreases with time, whereas for $N_d = 50\,\mathrm{cm}^{-3}$ the total longwave cooling is large enough to maintain cloud growth.

5.. Results - Simulations of the Diurnal Cycle

In general, shortwave heating decreases LWP and STBL-averaged TKE in stratocumulus as compared to nighttime cases (e.g., Turton and Nicholls 1987). Moreover, as heating strengthens during the morning cloud layer becomes at least partially decoupled from the surface, and this can also reduce TKE and LWP (e.g., Turton and Nicholls 1987; Lu and Seinfeld 2005; Sandu et al. 2008). Although these prior results are for larger LWP stratocumulus we find that shortwave heating has similar effects in our simulations (Fig. 3). For all N_d, LWP and cloud fraction decrease during the morning hours as the cloud layer warms and decouples from the sub-cloud layer (Fig. 3a). Production of drizzle and STBL-averaged TKE are

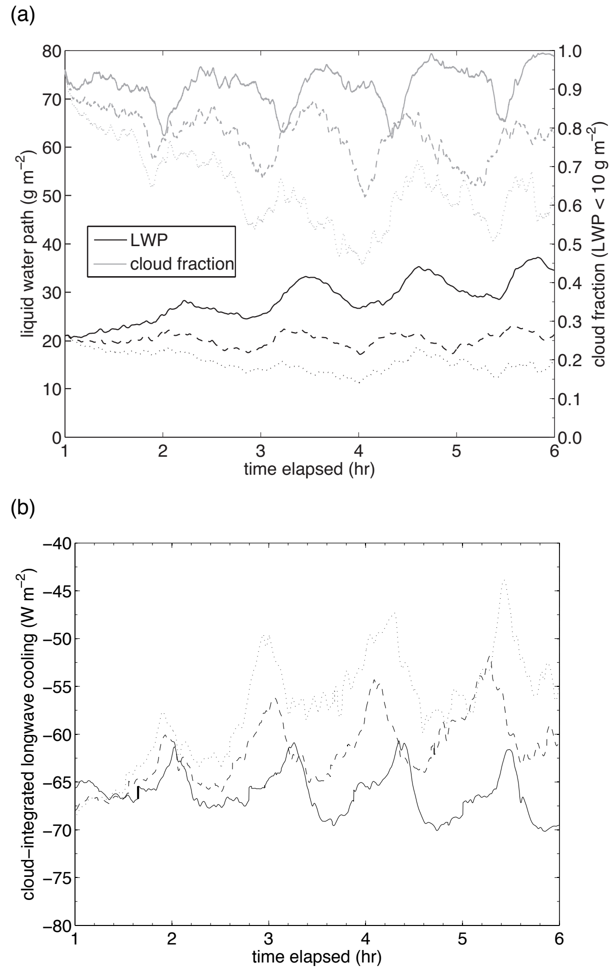

FIG. 2. Large-eddy output for six hour nocturnal simulations. N_d is held constant in each simulation at the values of $50\,\mathrm{cm}^{-3}$, $200\,\mathrm{cm}^{-3}$ and $1000\,\mathrm{cm}^{-3}$. These values of N_d are represented by the full, dashed and dotted lines, respectively. Time series of quantities are domain averaged and vertically integrated.

concomitantly reduced (Table 1).

Reductions in LWP and cloud fraction are also associated with decreases in total longwave cooling (Fig. 3b) because longwave cooling is sensitive to these reductions when LWP is low. The combination of increased shortwave warming and reduced longwave cooling consequently leads to strong reductions in LWP and in STBL-averaged TKE as N_d rises (Table 1). Shortwave warming also causes some decoupling of the cloud layer from the atmosphere below which reduces fluxes of vapor into the cloud. The reduction in vapor flux from below and the reduction in overall cloud radiative cooling allow for greater net evaporation of the cloud through entrainment. Liquid water path and longwave cooling are further reduced causing the cloud layer to thin and break. *These processes define a negative feedback loop for low LWP stratiform clouds causing either substantial reductions in LWP* ($N_d = 50\,\mathrm{cm}^{-3}$) *or the dissipation of the cloud layer when N_d is increased* ($N_d = 200\,\mathrm{cm}^{-3}$ and $1000\,\mathrm{cm}^{-3}$).

Similar to the nocturnal simulations, differences in entrainment play a vital role in the evolution of the daytime simu-

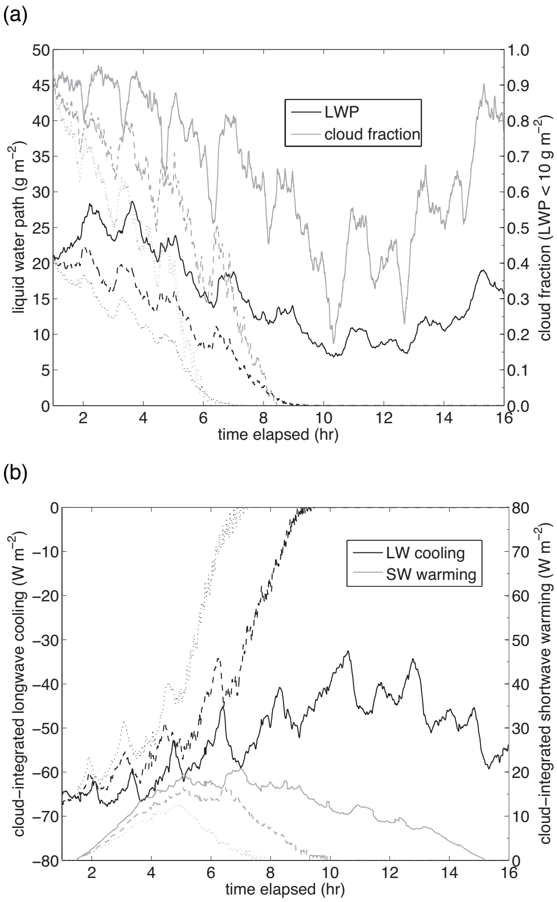

FIG. 3. Large-eddy output for sixteen hour simulations of the diurnal cycle. N_d is held constant in each simulation at the values of $50\,\mathrm{cm}^{-3}$, $200\,\mathrm{cm}^{-3}$ and $1000\,\mathrm{cm}^{-3}$. These values of N_d are represented by the full, dashed and dotted lines, respectively. Time series of quantities are domain averaged and vertically integrated.

lations. Initially shortwave warming is weak, and evaporation due to initial entrainment increases with N_d. Hence as N_d increases we find larger initial decreases in cloud fraction and LWP, similar to our nocturnal simulations. For the two larger concentrations ($N_d = 200\,\mathrm{cm}^{-3}$ and $1000\,\mathrm{cm}^{-3}$) total longwave cooling is reduced enough during the morning hours such that the cloud layer can not be maintained against further shortwave warming. For the lower concentration ($N_d = 50\,\mathrm{cm}^{-3}$), however, total longwave cooling remains sufficiently strong so that the cloud is be maintained against shortwave warming.

The dependency of shortwave warming on N_d (Fig. 1 does not appear to play an important role in the evolution of these daytime simulations. Nevertheless, the LWP and cloud fraction vary more widely with N_d in our daytime simulations as compared to our nocturnal simulations. This indicates a stronger aerosol response for low LWP clouds during the daytime hours.

6.. Summary and Concluding Remarks

To test the robustness of our results we conducted ensembles of nocturnal and daytime simulations. We ran six additional realizations for each pair of droplet concentration ($N_d = 50\,\mathrm{cm}^{-3}$ and $1000\,\mathrm{cm}^{-3}$) and nighttime/daytime conditions, resulting in 24 additional simulations. We created these ensembles by perturbing the initial temperature field differently in each realization. All members of these ensembles displayed the same important qualitative features as described in the two previous sections, suggesting that our results are robust.

Our simulations suggest that increasing droplet concentration in low LWP stratiform clouds leads to decreases in LWP and possibly cloud dissipation, in contrast to the hypothesis of Albrecht (1989). The mechanism for this decrease in LWP is unlike that of Ackerman et al. (2004). Their study determined that increasing N_d leads to slower sedimentation of cloud droplets as they become smaller. Entrainment of dry air from above the cloud top interface can then lead to more efficient drying of the cloud, reducing the LWP. Since we do not account for sedimentation of cloud droplets, and our cloud drop concentrations are constant, our mechanism is different.

In our study we find, for low LWP cloud layers, that changes in both entrainment drying and radiative heating with droplet concentration drive a second AIE. The evaporative-entrainment feedback leads to rapid initial entrainment and evaporation of the cloud layer when N_d is high. This efficient entrainment drying leads to more cloud breaks and lower LWP values for higher droplet concentrations. Because total longwave cooling is sensitive to LWP when LWP is low, there are consequent reductions in total longwave cooling and circulation strength. Therefore, for low values of LWP these cloud layers are more tenuous when droplet concentration is high and are more prone to dissipating during the day, and especially so when LWP $< 20\,\mathrm{g\,m}^{-2}$.

Perturbations in the aerosol concentrations of low-level, low LWP cloud layers can therefore substantially alter the radiative forcing of both the surface and atmosphere, and may have possible impacts on regional, and perhaps global, climate (Turner et al. 2007). An increase in aerosol can lead to increases in N_d, resulting in lower cloud LWP and cloud fractions, or even cloud dissipation. This change in cloud evolution with N_d is associated with reduced downwelling longwave flux at the surface during both nighttime and daytime (Table 2). Reductions in the longwave flux are more substantial during the daytime because LWP varies more with N_d. Increasing N_d from $50\,\mathrm{cm}^{-3}$ to $1000\,\mathrm{cm}^{-3}$ results in a 3% decrease in this flux during night and a 15% decrease during the day. The albedo of the cloud scene is also decreased as N_d increases and LWP and cloud fraction decrease.

Geographic regions where low LWP clouds are frequent and aerosol concentrations are relatively low, such as the Arctic (Curry et al. 1996; De Boer et al. 2009), may be particularly susceptible to changes in aerosol concentrations. Francis and Hunter (2006) suggest that downwelling longwave flux at the surface plays a prominent role in the retreat or advance of the Arctic sea-ice edge. Moreover, Kay et al. (2008) showed that the 2007 minimum in sea-ice extent was related to cloud cover. It is quite possible that aerosol-induced changes in

Arctic cloud cover could have important ramifications for the energy budget of the Arctic surface. We model warm clouds in this study, and clouds in the Arctic are liquid phase during much of the warm season (Curry et al. 1996). However, the importance of this AIE with respect to ice and mixed-phase cloud processes in the Arctic should be investigated.

In general the global frequency of low-level, low LWP clouds will determine the importance of any attendant aerosol feedbacks to the radiative budget. Further examination of ground-based and satellite remote sensing data to determine the geographic and temporal frequency of low LWP clouds seems required.

Acknowledgement This research was supported by the Department of Energy's (DOE) Atmospheric Radiation Measurement Program, the National Aeronautics and Space Administration and the Pennsylvania Space Grant Consortium Research Fellowship Program. Computer resources were provided by the SHARCNET, a consortium of Canadian academic institutions.

References

Ackerman, A. S., M. P. Kirkpatrick, D. E. Stevens, and O. B. Toon, 2004: The impact of humidity above stratiform clouds on indirect aerosol climate forcing. *Nature*, **432**, 1014–1017.

Albrecht, B. A., 1989: Aerosols, cloud microphysics and fractional cloudiness. *Science*, **245**, 1227–1230.

Boers, R. and R. M. Mitchell, 1994: Absorption feedback in stratocumulus clouds: Influence on cloud top albedo. *Tellus*, **46A**, 229–241.

Bretherton, C. S., M. MacVean, P. Bechtold, A. Chlond, W. Cotton, J. Cuxart, H. Cuijpers, M. Khairoutdinov, B. Kosovic, D. Lewellen, C. Hoh Moeng, P. Siebesma, B. Stevens, D. Stevens, I. Sykes, and M. Wyant, 1999: An intercomparison of radiatively-driven entrainment and turbulence in a smoke cloud, as simulated by different numerical models. *Quart. J. Roy. Meteor. Soc.*, **125**, 391–423.

Bretherton, C. S., T. Uttal, C. W. Fairall, S. E. Yuter, R. A. Weller, D. Baumgardner, K. Comstock, R. Wood, and G. B. Raga, 2004: The EPIC 2001 stratocumulus study. *Bull. Amer. Meteor. Soc.*, **85**, 967–977.

Brunke, M. A., S. P. D. Szoeke, P. Zuidema, and X. Zeng, 2010: A comparison of ship and satellite measurements of cloud properties in the southeast Pacific stratus deck. *Atmos. Chem. Phys. Diss.*, **10**, 3301–3318.

Chen, T., W. B. Rossow, and Y. Zhang, 2000: Radiative effects of cloud-type variations. *J. Climate*, **13**, 264–286.

Coakley, J. A., R. L. Bernstein, and P. A. Durkee, 1987: Effect of ship-stack effluents on cloud reflectivity. *Science*, **237**, 1020–1022.

Cole, J. N. S., 2005: *Assessing the importance of unresolved cloud-radiation interactions in atmospheric global climate models using the multiscale-modelling framework.*. Ph.D. thesis, The Pennsylvania State University, State College, PA 16801, USA, 157 pp.

Cotton, W., R. Pielke, R. Walko, G. Liston, C. Tremback, J. Harrington, and H. Jiang, 2003: Rams 2000: Current status and future directions. *Meteor. Atmos. Phys.*, **82**, 5–29.

Curry, J. A., W. B. Rossow, D. Randall, and J. L. Schramm, 1996: Overview of arctic cloud and radiation characteristics. *J. Climate*, **9**, 1731–1764.

De Boer, G., E. W. Eloranta, and M. D. Shupe, 2009: Arctic mixed-phase stratiform cloud properties from multiple years of surface-based measurements at two high-latitude locations. *J. Atmos. Sci.*, **66**, 2874–2887.

Durkee, P. A., K. J. Noone, and R. T. Bluth, 2000: The Monterey Area Ship Track Experiment. *J. Atmos. Sci.*, **57**, 2523–2541.

Francis, J. A. and E. Hunter, 2006: New insight into the disappearing Arctic sea ice. *Eos Trans. AGU*, **87**, 509–511.

Garrett, T. J. and C. Zhao, 2006: Increased arctic cloud longwave emissivity associated with pollution from midlatitudes. *Nature*, **440**, 787–789.

Harrington, J., 1997: *The Effects of Radiative and Microphysical Processes on Simulated Warm and Transition Season Arctic Stratus*. Ph.D. thesis, Colorado State University, Ft. Collins CO, 80523, USA.

Harrington, J. Y. and P. Q. Olsson, 2001: A method for the parameterization of cloud optical properties in bulk and bin microphysical models: Implications for arctic cloudy boundary layers. *Atmos. Res.*, **57**, 51–80.

Hartman, C. and J. Harrington, 2005: Radiative impacts on the growth of drops in simulated stratocumulus. Part I: Strong solar heating. *J. Atmos. Sci.*, **62**, 2323–2338.

Hill, A. A., S. Dobbie, and Y. Yin, 2008: The impact of aerosols on non-precipitating marine stratocumulus. I: Model description and prediction of the indirect effect. *Quart. J. Roy. Meteor. Soc.*, **134**, 1143–1154.

Hill, A. A., G. Feingold, and H. Jiang, 2009: The influence of entrainment and mixing assumption on aerosol-cloud interactions in marine stratocumulus. *J. Atmos. Sci.*, **66**, 1450–1464.

Jiang, H., G. Feingold, and W. R. Cotton, 2002: Simulations of aerosol-cloud-dynamical feedbacks resulting from entrainment of aerosol into the marine boundary layer during the Atlantic stratocumulus transition experiment. *J. Geophys. Res.*, **107**, doi:10.1029/2001JD001502.

Kay, J. E., T. L'Ecuyer, A. Gettelman, G. Stephens, and C. O'Dell, 2008: The contribution of cloud and radiation anomalies to the 2007 Arctic sea ice extent minimum. *Geophys. Res. Let.*, **35**, doi:10.1029/2008GL033451.

Klein, S. A. and D. L. Hartmann, 1993: The seasonal cycle of low stratiform clouds. *J. Climate*, **6**, 1587–1606.

Lee, S. S., J. E. Penner, and S. M. Saleeby, 2009: Aerosol effects on liquid-water path of thin stratocumulus clouds. *J. Geophys. Res.*, **114**, doi:10.1029/2008JD010513.

Lilly, D. K., 1968: Models of cloud topped mixed layers under a strong inversion. *Quart. J. Roy. Meteor. Soc.*, **94**, 292–309.

Lu, M.-L., W. C. Conant, H. H. Jonsson, V. Varutbangkul, R. C. Flagan, and J. H. Seinfeld, 2007: The Marine Stratus/Stratocumulus Experiment: aerosol-cloud relationships in marine stratocumulus. *J. Geophys. Res.*, **112**, doi:10.1029/2006JD007985.

Lu, M.-L. and J. H. Seinfeld, 2005: Study of the aerosol indirect effect by large-eddy simulation of marine stratocumulus. *J. Atmos. Sci.*, **62**, 3909–3932.

McClatchey, R., R. Fenn, J. Selby, F. Voltz, and J. Garing, 1972: *Optical Properties of the Atmosphere. 3rd ed. AFCRL-72-0497*. Air Force Cambridge Research Laboratories, Bedford, MA, 108 pp.

Meyers, M. P., R. L. Walko, J. Y. Harrington, and W. R. Cotton, 1997: New rams cloud microphysics parameterization. Part II: The two-moment scheme. *Atmos. Res.*, **45**, 3–39.

Miles, N. L., J. Verlinde, and E. E. Clothiaux, 2000: Cloud droplet size distributions in low-level stratiform clouds. *J. Atmos. Sci.*, **57**, 295–311.

Nicholls, S., 1984: The dynamics of stratocumulus: Aircraft observations and comparisons with a mixed layer model. *Quart. J. Roy. Meteor. Soc.*, **110**, 783–820.

Petters, J. L., 2009: *The Impact of Radiative Heating and Cooling on Marine Stratocumulus Dynamics.*. Ph.D. thesis, The Pennsylvania State University, State College, PA 16801, USA, 161 pp.

Randall, D., S. Bony, R. Colman, T. Fichefet, J. Fyfe, V. Kattsov, A. Pitman, J. Shukla, J. Srinivasan, R. Stouffer, A. Sumi, and K. Taylor, 2007: *Climate Change 2007: The Physical Science Basis, Contribution of Working Group I to the Fourth Assessment Report of the Intergovernmental Panel on Climate Change*, Cambridge University Press, Cambridge, chapter Climate models and their evaluation. S. Solomon and coeditors.

Ritter, B. and J.-F. Geleyn, 1992: A comprehensive radiation scheme for numerical weather prediction models with potential applications in climate simulations. *Mon. Wea. Rev.*, **120**, 303–325.

Sandu, I., J.-L. Brenguier, O. Geoffroy, O. Thouron, and V. Masson, 2008: Aerosol impacts on the diurnal cycle of marine stratocumulus. *J. Atmos. Sci.*, **65**, 2705–2718.

Stevens, B., W. R. Cotton, G. Feingold, and C.-H. Moeng, 1998: Large-eddy simulations of strongly precipitating, shallow, stratocumulus-topped boundary layers. *J. Atmos. Sci.*, **55**, 3616–3638.

Turner, D. D., A. M. Vogelmann, R. T. Austin, J. C. Barnard, K. Cady-Pereira, J. C. Chiu, S. A. Clough, C. Flynn, M. M. Khaiyer, J. Liljegren, K. Johnson, B. Lin, C. Long, A. Marshak, S. Y. Matrosov, S. A. McFarlane, M. Miller, Q. Min, P. Minnis, W. O'Hirok, Z. Wang, and W. Wiscombe, 2007: Thin liquid water clouds: their importance and their challenge. *Bull. Amer. Meteor. Soc.*, **88**, 177–190.

Turton, J. D. and S. Nicholls, 1987: A study of the diurnal variation of stratocumulus using a multiple mixed layer model. *Quart. J. Roy. Meteor. Soc.*, **113**, 969–1009.

Twomey, S. A., 1977: The influence of pollution on the shortwave albedo of clouds. *J. Atmos. Sci.*, **34**, 1149–1152.

Wang, S., Q. Wang, and G. Feingold, 2003: Turbulence, condensation, and liquid water transport in numerically simulated nonprecipitating stratocumulus clouds. *J. Atmos. Sci.*, **60**, 262–278.

Wood, R., 2007: Cancellation of aerosol indirect effects in marine stratocumulus through cloud thinning. *J. Atmos. Sci.*, **64**, 2657–2669.

Xu, K.-M. and D. A. Randall, 1995: Impact of interactive radiative transfer on the macroscopic behavior of cumulus ensembles: Part I: radiation parameterization and sensitivity tests. *J. Atmos. Sci.*, **52**, 785–799.

Table 1. Horizontally and vertically averaged TKE and domain-averaged vertically integrated drizzle flux divergence, both temporally averaged over the fifth and sixth hours of each set of simulations.

	Nocturnal Simulations		Simulations of the Diurnal Cycle	
$N_d\,(\mathrm{cm}^{-3})$	TKE $(\mathrm{m}^2\,\mathrm{s}^{-2})$	Drizzle Flux $(\mathrm{W\,m}^{-2})$	TKE $(\mathrm{m}^2\,\mathrm{s}^{-2})$	Drizzle Flux $(\mathrm{W\,m}^{-2})$
50	0.053	6.3	0.028	3.3
200	0.035	1.1	0.021	0.7
1000	0.028	0.8	0.014	0.4

Table 2. Domain-averaged downwelling surface longwave flux and shortwave reflectivity (albedo) at top of modeling domain. For the nocturnal simulations fluxes are temporally averaged over the last two hours of simulation. For the simulations of the diurnal cycle data are temporally averaged over the seventh and eighth hours of simulation, when the sun is highest in the sky.

	Nocturnal Simulations	Simulations of the Diurnal Cycle	
$N_d\,(\mathrm{cm}^{-3})$	Longwave Flux $(\mathrm{W\,m}^{-2})$	Longwave Flux $(\mathrm{W\,m}^{-2})$	Albedo
50	368.5	352.8	0.13
200	363.0	319.4	0.08
1000	357.7	300.0	0.04